Journal of Radioanalytical and Nuclear Chemistry (2023) 332:3911–3918
https://doi.org/10.1007/s10967-023-09118-6

Study on the uranium adsorption and reusability characteristics of amidoximated polypropylene-acrylonitrile-acrylic acid fibrous adsorbent

Jong-Gil Im[1] · Ho-Song Pak[1] · Un-Chol Jon[1] · Song-Bom Ri[1] · Sun-Yong Om[1] · Chol-Jin Jong[1]

Received: 15 March 2023 / Accepted: 13 August 2023 / Published online: 30 August 2023

Abstract
The kinetics and thermodynamics of the U(VI) adsorption process on amidoximated polypropylene-acrylonitrile-acrylic acid (AOPP-AN-AAc) fiber adsorbent were investigated by static adsorption at different temperatures. The process of uranium adsorption by the adsorbent was fitted to the pseudo-second-order kinetic model and the pseudo-second-order rate constant and the pseudo activation energy at different temperatures were determined. The thermodynamic properties of the U(VI) adsorption process by the adsorbent were also evaluated. The optimum conditions of adsorption were determined by studying the effects of U(VI) concentration, solution pH, temperature and stirring conditions on the adsorption equilibrium. The desorption and regeneration properties of U(VI) adsorbed on the adsorbent were evaluated in different media.

Keywords Fibrous adsorbent · Adsorption properties and kinetics · Amidoxime · Reusability · Uranium · Seawater

Introduction

Seawater is a solution of rare metals such as uranium and vanadium with a concentration of about ppb, for example, the amount of uranium is 4.5 billion tones, which is equal to 1,000 times that of terrestrial uranium [1]. Thus, seawater can be a major resource of uranium.

Therefore, the recovery of rare metals such as uranium from seawater was considered as one of the useful technologies for energy security of nuclear power plants in the future. The concentration of uranium in seawater was 3.3 µg/L [2], and the pH was 7.5–8.3 [3, 4]. The low concentration of uranium in seawater and the high concentration of ions coexisting with uranium make it difficult to separate uranium selectively. Uranium is present in various forms, including $UO_2(CO_3)_3^{4-}$, $UO_2(OH)_3^-$, $UO_2(CO_3)_2^{2-}$, UO_2^{2+}, $UO_2(OH)^+$, $UO_2(OH)_2$, where $UO_2(CO_3)_3^{4-}$ (84.9%) is the most abundant in seawater [5].

Many authors have conducted a number of studies on the recovery of uranium from seawater using various organic adsorbents, including fibrous adsorbent with excess amidoxime groups, PP (polypropylene) grafted with the amidoxime group adsorbent, fibrous amidoxime adsorbents (acrylonitrile) and methacrylic acid and subsequent amidoximation [6–12]. Previous studies have investigated the kinetic and thermodynamic studies of uranium adsorption processes of adsorbents containing amidoxime functional groups, the effects of pH and other factors on selectivity and adsorption and regeneration [13–15]. The results of reported studies showed that adsorbents containing amidoxime functional groups have high selectivity for U(VI) and high adsorption capacity at the pH of sea water. Therefore, adsorbents containing amidoxime chelate groups are considered to be the most promising for uranium recovery from seawater in the near future.

In this paper, the kinetics, thermodynamic properties and the influence of factors on U(VI) adsorption and reproducibility of amidoximated polypropylene-acrylonitrile-acrylic acid (AOPP-AN-AAc) fibrous adsorbent synthesized by pre-irradiated method for efficient recovery of U(VI) from seawater were investigated.

✉ Ho-Song Pak
ener4@ryongnamsan.edu.kp

[1] Energy Science College of Kim Il Sung University, Pyongyang, Democratic People's Republic of Korea

Experimental method

Reagents

The AOPP-AN-AAc fiber adsorbents used in this study were synthesized by oxidization with hydroxylamine after co-grafting of acrylonitrile and acrylic acid (PP-AN-AAc fibers) in pre-irradiated polypropylene.

Uranium solution used in experiments was prepared by diluting a solution containing 5000 ppm of uranyl tricarbonate ion ($UO_2(CO_3)_3]^{4-}$) to the corresponding concentration.

All reagents such as NaCl, KCl, $CaCl_2$, $MgCl_2$, HCl, $NaHCO_3$, Na_2CO_3 etc. used in this study were analytical grade and used with no further purification.

Instrument

Spectrophotometer (SP-752PC, China).

Methods

The U(VI) adsorption experiments were carried out by adding 0.1 g of AOPP- AN-AAc fiber adsorbent in 50 mL U(VI) solution and determining the concentration of U(VI) of the solution after reaching equilibrium at a given temperature, time and agitation rate.

Influence of pH for U(VI) adsorption have been investigated in U(VI) concentrations of 25 mg·L^{-1} and the pH values from pH 3.0 to 9.0.

The pH values in solutions containing U(VI) were adjusted using dilute hydrochloric acid or Na_2CO_3, respectively, and finally controlled with two kinds of conventional buffer solutions, CH_3COOH-CH_3COONa and $Na_2B_4O_7$-H_3BO_3.

In 50 mL of aqueous solution (pH 8) with initial U(VI) concentration of 25 mg L^{-1}, 0.1 g of fiber adsorbent was added and the amount of adsorbed U(VI) was determined by determining the U(VI) concentration of the aqueous solution with the adsorption time, with stirring at 180 rpm at different temperatures.

The effect of coexisting ions was evaluated by adsorption of U(VI) in a solution mixed with a solution of U(VI) and a solution with twice the concentration of metal ions (55.0 g·L^{-1} NaCl, 10.4 g·L^{-1} $MgCl_2$, 2.34 g L^{-1} $CaCl_2$, 1.45 g·L^{-1} KCl) in seawater. Desorption experiments of U(VI) on the adsorbent were performed to evaluate the desorption rate by immersing 0.1 g of the adsorbent with U(VI) ions adsorbed at 20 °C in 100 mL of different concentration of the desorber solution (acidic solution and alkaline solution) and determining the concentration of U(VI) with time under stirring at 180 rpm.

Experiment for the regenerative evaluation of the AOPP-AN-AAc fiber adsorbent was conducted by considering the change in uranium adsorption amount, repeating the operation of desorption with 100 mL of 0.5 mol·L^{-1} HCl solution after 2 h of adsorption with 0.1 g of fibrous adsorbent in 50 mL (pH 8) aqueous solution of 25 mg·L^{-1} initial U(IV) concentration and stirring at 180 rpm at 20 °C.

In all experiments, the concentration of U(VI) of the solution was determined by the Arsenazo(III) colorimetric method (wavelength of maximum absorption; 656 nm). The amount of adsorption(q_e) was determined by the following equation.

$$q_e = \frac{(C_0 - C_e)\Delta V}{m} (\text{mg/g}) \quad (1)$$

where C_0 and C_e are the initial concentrations of U(VI) in aqueous solution and the concentrations of U(VI) after equilibration (mg·L^{-1}), V is the volume of aqueous solution (L), and m is the mass of AOPP-AN-AAc fiber adsorbent (g), respectively.

Results and discussions

U(VI) adsorption kinetics

The variation of U(VI) adsorption amount with time on the AOPP-AN-AAc fiber adsorbent are shown in Fig. 1.

As shown in Fig. 1, equilibrium at 20 °C was reached within about 50 min when the concentration of initial U (VI) solution was 25, 50, and 100 mg·L^{-1}. The time taken to adsorb 50% was about 6.8 min for three initial concentrations of U (VI) solution.

In order to determine the adsorption rate and validate the kinetic mechanisms governing the adsorption process, the

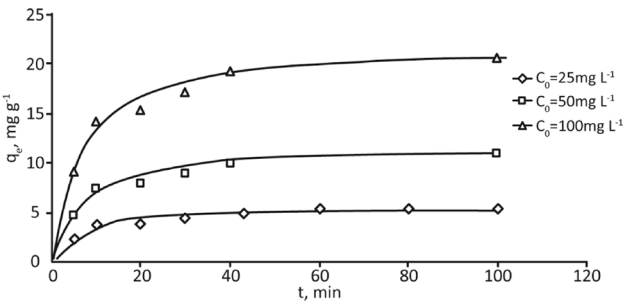

Fig. 1 Variation of adsorption amount with adsorption time in different initial U(VI) aqueous solutions. (U(VI) solution volume: 50 mL, pH 8, adsorbent volume 0.1 g, temperature: 20 °C, stirring speed: 180 rpm)

pseudo-first-order kinetic model, the pseudo-second-order kinetic model, was used to explain the kinetic process. These models are most used to account for heavy metal adsorption on sorbents, including chelate resins.

The pseudo-first-order kinetic model is based on the fact that the adsorption rate of the adsorbate on the adsorbent depends on the amount of adsorbate.

The pseudo-first-order kinetic model can be written as follows.

$$\frac{dq_t}{dt} = k_1 \cdot \left(q_e + q_t\right) \tag{2}$$

where k_1 is the pseudo first-order rate constant (min^{-1}), q_e and q_t are the adsorption amount ($mg{\cdot}g^{-1}$) of U(VI) at equilibrium state and time (min).

Integrating at the initial condition of t = 0, $q_t = 0$, we can obtain the following linear relationship.

$$\ln\left(q_e - q_t\right) = -k_1 \cdot \neq t + lnq_e \tag{3}$$

The values of the pseudo-first-order rate constants and the values calculated from the plot (Fig. 2) between $\ln\left(q_e - q_t\right)$ and t are given in Table 1.

The pseudo-second order kinetic model can be written following;

$$\frac{dq_t}{dt} = k_2 \cdot (q_e + q_t)^2 \tag{4}$$

where k_2 is the pseudo-second-order rate constant ($g{\cdot}mg^{-1}{\cdot}min^{-1}$).

Integrating at t = 0 at the initial condition of $q_t = 0$ gives the following expression.

$$\frac{t}{q_t} = \frac{1}{k_1 \cdot q_e^2} + \frac{t}{q_e} \tag{5}$$

The linear form of the pseudo-second-order kinematic model, the plot between $\frac{t}{q_t} - t$, is shown in Fig. 3.

The values of the pseudo-second-order rate constants and q_e calculated from the plot between $\frac{t}{q_t} - t$ were given in Table 1.

As shown in Table 1, the experimentally determined adsorption amount ($q_{e,exp}$) in equilibrium is not consistent with the equilibrium adsorption amount ($q_{e,cal}$) calculated from the pseudo-first-order kinetic model, especially with the value of the correlation coefficient of 0.96, it can be seen that the adsorption process does not match the pseudo-first-order kinetics, so that the adsorption process is not diffusion rate, especially the durability.

However, the equilibrium adsorption amount calculated from the pseudo-second-order kinetic model is comparatively good with the experimentally determined adsorption amount and the correlation coefficient is 0.99, indicating that the adsorption process is suitable for the pseudo-second-order kinetic model.

Based on the pseudo-second-order kinetics, the time taken to reach 50% of the adsorption amount from Eq. (6)

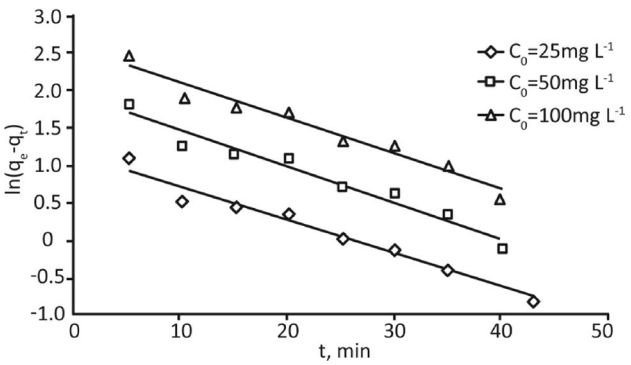

Fig. 2 Pseudo first-order kinematics model

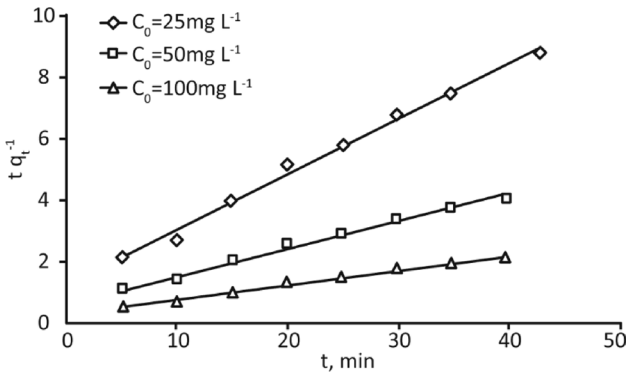

Fig. 3 Pseudo second-order kinematics model

Table 1 Pseudo first-order kinetics and pseudo-second-order kinetic constants (293 K)

$C_0(mg{\cdot}L^{-1})$	$q_{e,exp}$ ($mg{\cdot}g^{-1}$)	pseudo-first-order kinetic model			pseudo-second-order kinetic model		
		k_1 (min^{-1})	$q_{e,cal}$ ($mg{\cdot}g^{-1}$)	R^2	k_2 ($g{\cdot}mg^{-1}{\cdot}min^{-1}$)	$q_{e,cal}$ ($mg{\cdot}g^{-1}$)	R^2
25	5.40	0.045	3.23	0.9611	0.0267	5.59	0.9937
50	10.85	0.047	6.77	0.9519	0.0128	11.31	0.9918
100	20.70	0.047	12.78	0.9497	0.0069	21.51	0.9920

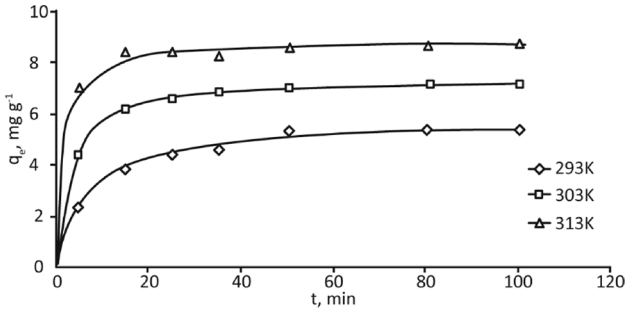

Fig. 4 Variation of adsorption amount with adsorption time at different temperatures. (U(VI) concentration: 25 mg L^{-1}, solution volume: 50 mL, pH 8, sorbent volume: 0.1 g, stirring speed: 180 rpm)

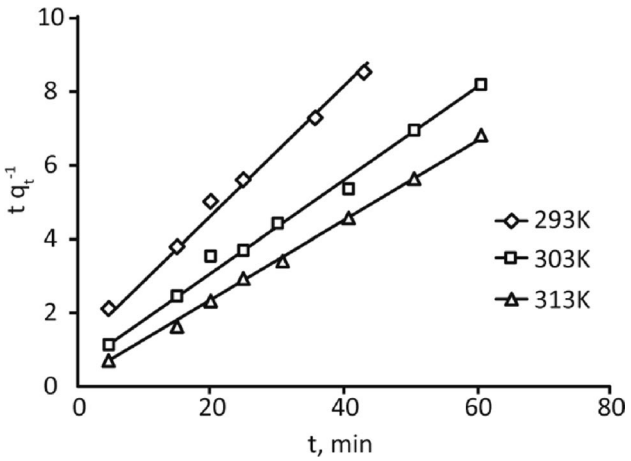

Fig. 5 Relationship between different temperatures

was calculated as 6.7, 6.9 and 6.8 min for initial U(VI) concentrations of 25, 50 and 100 mg L^{-1}, respectively.

$$t_{1/2} = \frac{1}{k_2 \cdot q_e} \tag{6}$$

Variation of adsorption amount with adsorption time at different temperatures is shown in Fig. 4.

From the linear form of the pseudo-second-order kinematic model, the rate constants were determined by the plot between t/q_t and t (Fig. 5) at different temperatures.

Based on Arrhenius equation (Eq. 7), the pseudo activation energy was determined from the $\frac{t}{q_t} - t$ plot (Fig. 6).

$$\ln k = \ln A - \frac{E_a}{R} \cdot \frac{1}{T} \tag{7}$$

where k is the pseudo-second-order rate constant (g·mg^{-1}·min^{-1}), A is the frequency factor, Ea is the pseudo activation energy (kJ·mol^{-1}), T is the

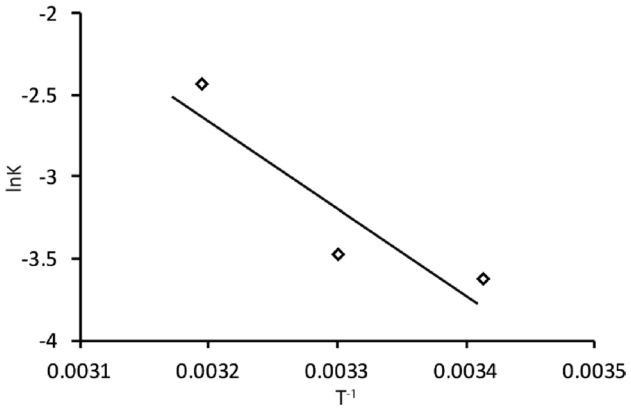

Fig. 6 Relationship between lnk − $\frac{1}{T}$

Table 2 Pseudo second-order rate constant and pseudo activation energy

Temperature (K)	k (g·mg^{-1}·min^{-1})	E_a (kJ·mol^{-1})
293	0.0267	44.9
303	0.0310	
313	0.0876	

absolute temperature (K), and R is the gas universal constant (8.314×10^{-3} kJ·mol^{-1}·K^{-1}).

The pseudo-second-order rate constants and pseudo activation energies determined at different temperatures were given in Table 2.

As shown in Table 2, since the pseudo activation energy was calculated as 44.9 kJ·mol^{-1}, the U(VI) adsorption process on the AOPP-AN-AAc fiber adsorbent could be considered as chemisorption.

Adsorption thermodynamics

Considering the thermodynamics of the U(VI) adsorption process by the AO PP-AN-AAc fiber adsorbent was very important to evaluate the feasibility and spontaneous nature of the adsorption process.

There were the following relationships between thermodynamic factors such as enthalpy change, entropy change, and Gibbs energy change that reflect the spontaneous nature of the adsorption process.

$$\Delta G^0 = -RTlnk_d \tag{8}$$

$$\Delta G^0 = \Delta H^0 - T \cdot \Delta S^0 \tag{9}$$

where $\Delta H^0, \Delta S^0$ and ΔG^0 are the standard enthalpy changes(kJ mol^{-1}), standard entropy changes(J mol^{-1} K^{-1}),

Table 3 Distribution coefficient of U(VI) in sorbent and aqueous phase at different temperatures

Temperature (K)	q_e(mg·g^{-1})	C_e(mg·mL^{-1})	K_d
283	3.7	0.0176	218.4
293	5.4	0.0142	380.3
303	7.25	0.0105	690.5
313	8.85	0.0073	1212.3

Table 4 Thermodynamic parameters of adsorption process at different temperatures

Temperature (K)	ΔG^0 (kJ·mol^{-1})	ΔH^0 (kJ·mol^{-1})	ΔS^0 (J·mol^{-1}·K^{-1})
283	− 12.6	42.2	193.8
293	− 14.6		
303	− 16.5		
313	− 18.4		

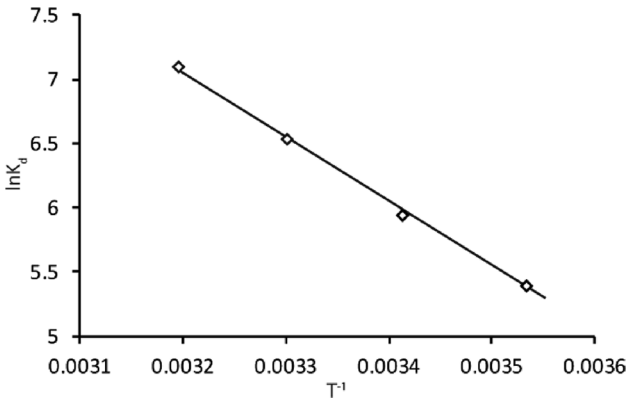

Fig. 7 Relationship curve between $\ln k_d - \frac{1}{T}$

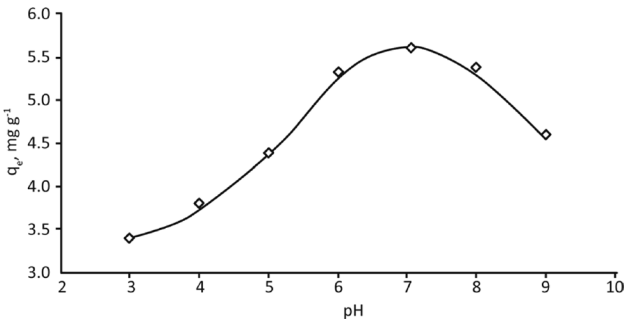

Fig. 8 Variation of adsorption amount with pH. (U(VI) concentration: 25 mg L^{-1}, solution volume: 50 mL, sorbent volume: 0.1 g, temperature: 20 °C, time: 2 h, stirring speed: 180 rpm)

and standard Gibbs energy changes(kJ mol^{-1}) during adsorption, respectively, and K_d is the adsorption equilibrium distribution coefficient.

From (8) and (9), the following relation holds.

$$\ln k_d = -\frac{\Delta H^0}{R} \cdot \frac{1}{T} + \frac{\Delta S^0}{R} \tag{10}$$

The distribution coefficient of U(VI) between adsorbent and aqueous phase in equilibrium was determined from the following equation.

$$k_d = \frac{q_{e(mg/g)}}{C_e(mg/mL)} \tag{11}$$

The distribution coefficients of U(VI) in AOPP-AN-AAc fiber adsorbents and aqueous phase at different temperatures were given in Table 3.

ΔH^0, ΔS^0 is calculated from the slope and section of the plot between $\ln k_d - \frac{1}{T}$ (Fig. 7) and the values of the thermodynamic parameters were given in Table 4.

The positive value of ΔH^0 (42.2 kJ·mol^{-1}) indicates that the adsorption process was endothermic and that the U(VI) adsorption process was favored at higher temperatures. Also, since the ΔH^0 value was above 40 kJ·mol^{-1}, a strong interaction between U(VI) ions and AOPP-AN-AAc fiber sorbent was shown, indicating that the adsorption process was chemisorption. The positive value of ΔS^0(193.8 J·mol^{-1}·K^{-1}) indicated that the disorder at the solid–liquid interface increased during the adsorption of U(VI) ions on the adsorbent. Thus, it could be seen that when the adsorption process occurred spontaneously, i.e. when $\Delta H^0 < T\Delta S^0$, the entropy change should be considered more than the enthalpy change of the adsorption process. The negative values of ΔG^0 calculated at different temperatures indicate that the adsorption process of U(VI) ions on the sorbent occurs spontaneously over the temperature range at which the experiments were carried out.

Effect of pH on the adsorption of U(VI)

The pH effect on the sorption amount of uranium qe by AOPP-AN-AAc fiber sorbent was investigated in the range of pH 3–9. Figure 8 shows the variation of uranium adsorption amount with pH.

As shown in Fig. 8, the increase in uranium adsorption with increasing pH from 3 to 7 can be attributed to the decrease in the concentration of H^+ ions and the predominant cation species of UO_2^{2+}. Thus, the adsorption amount of uranium increases with pH between pH 3–7. Above pH 8, the U adsorption decreases, which may be due to the hydrolysis of UO_2^{2+} in weak base solution to form precipitates such as $UO_2(OH)_2$, i.e., amidoxime groups

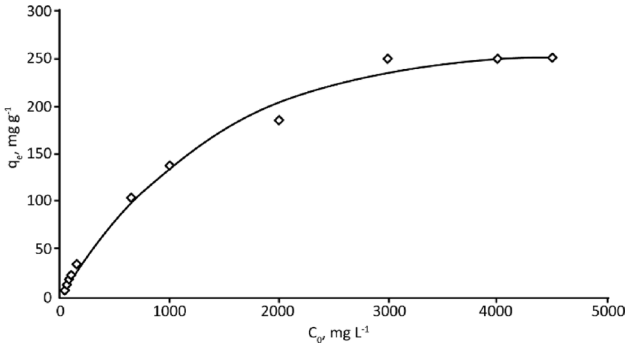

Fig. 9 Variation of adsorption amount with initial U (VI) concentration. (solution volume: 50 mL, pH 8, adsorbent: 0.1 g, temperature: 20 °C, time: 2 h, stirring speed: 180 rpm)

interact effectively with uranyl cations but not with uranyl hydroxide. Therefore, the optimum acidity was determined to be pH 6.0–8.0.

Effect of initial U(VI) concentration

The variation of the adsorption amount with initial U (VI) concentration was shown in Fig. 9.

As shown in Fig. 9, the adsorption amount of U (VI) at equilibrium was less than 250 mg·g^{-1}, which increases rapidly with increasing initial U (VI) concentration, and was hardly affected by the initial U (VI) concentration above 2500 mg·L^{-1}.

The increase in adsorption amount with increasing initial U (VI) concentration was due to the large number of adsorption active sites on the adsorbent at this temperature, and when the adsorption amount was 250 mg·g^{-1}, the adsorption active sites almost reach saturation and were almost unaffected by the initial concentration.

In particular, when the initial U (VI) concentration was 20–100 mg·L^{-1}, the adsorption amount increases almost linearly with the increase of the initial concentration, due to the large number of adsorption active sites remaining on the adsorbent compared to the amount of U (VI) in the solution.

Effect of temperature

The variation of adsorption amount with temperature was shown in Fig. 10.

As shown in Fig. 10, the adsorption amount increases with increasing temperature.

This may be due to the large number of adsorption active sites present in the adsorbent in the range of the initial U (VI) amount tested.

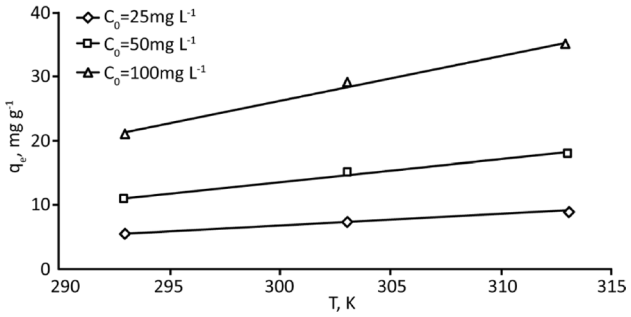

Fig. 10 The variation of adsorption amount with temperature

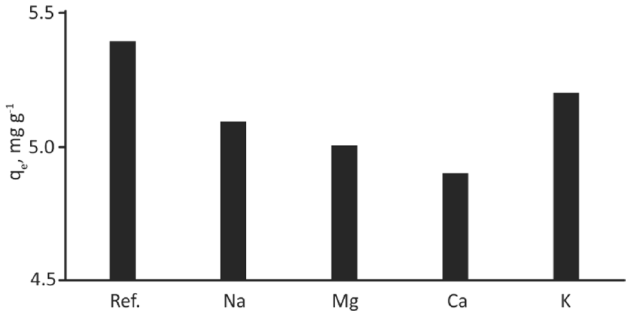

Fig. 11 Effect of coexisting ions on the adsorption amount of U(VI). (Initial [U(VI)] = 25 mg·L^{-1}, [Na^+] = 10.8 g·L^{-1}, [Mg^{2+}] = 1.33 g·L^{-1}, [Ca^{2+}] = 0.422 g·L^{-1}, [K^+] = 0.380 g·L^{-1})

Table 5 Variation of U (VI) adsorption amount with stirring speed

Stirring speed (rpm)	60	100	120	150
U (VI) adsorption amount (mg·g^{-1})	4.8	5.2	5.3	5.35

Effect of coexisting ions

The effect of coexisting ions on the adsorption amount of U(VI) was shown in Fig. 11.

As shown in Fig. 11, the order of influence on the adsorption of U (VI) was $Ca^{2+} > Mg^{2+} > Na^+ > K^+$. The slight decrease in U(VI) adsorption in the coexistence of Mg^{2+} and Ca^{2+} ions can be attributed to the reduction in the amount of U(VI) ions dissolved in the solution by the formation of $Mg_2[UO_2(CO_3)_3]$ and $Ca_2[UO_2(CO_3)_3]$ complexes.

Effect of stirring speed

The variation of U (VI) adsorption amount with stirring speed was shown in Table 5.

As shown in Table 3, the stirring speed was not significantly affected from 120 rpm above. At low stirring speed, the amount of adsorption decreases because external diffusion of uranyl ions to the adsorbent particle surface becomes

rate-limiting, and with increasing stirring speed, the thickness of the external diffusion layer decreases, leading to a higher external diffusion rate, which leads to saturation of the adsorbent. Therefore, the stirring speed was maintained as 180 rpm for the kinetic experiments.

Regeneration of adsorbent

Desorption characteristics of U(VI) on adsorbents with acidic and alkaline solution

The desorption characteristics of U(VI) adsorbed on the adsorbent were investigated. The desorption rates of UO_2^{2+} ions from the adsorbent with time were shown in Fig. 12, while different concentrations of $NaHCO_3$ and Na_2CO_3 solutions were used as desorbing agents.

As shown in Fig. 12, the higher the desorption rate (96.3% at 1 mol L^{-1}) was observed when Na_2CO_3 solution was used as desorber than $NaHCO_3$ solution at the same concentration, the higher the desorption rate was observed at higher Na_2CO_3 concentration. When 1 mol L^{-1} Na_2CO_3 solution was used as desorber, the time to reach saturation of desorption rate was about 75 min. The desorption rates of UO_2^{2+} ions from the adsorbent with time when different concentrations of HCl solutions were used as desorbing agents were shown in Fig. 13.

As shown in Fig. 13, it can be seen that the higher the concentration of HCl, the higher the desorption rate.

It can be seen that the acid solution used as desorbing agent has higher desorption rate and shorter desorption equilibrium time than the slightly alkaline solution.

Recovery of fiber adsorbent

The results of the seven-cycle desorption process of uranium onto the adsorbent with 100 mL of 0.5 mol L^{-1} HCl solution were shown in Fig. 14.

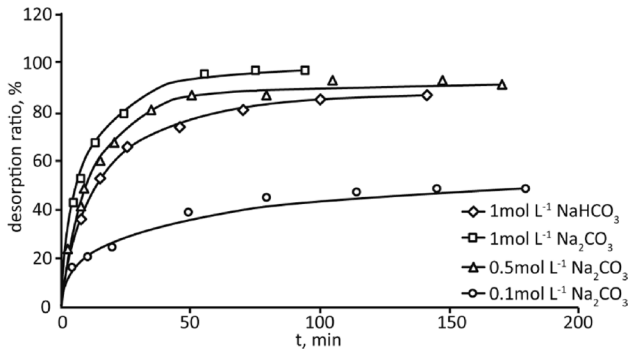

Fig. 12 Variation of desorption rate with time in different concentrations of $NaHCO_3$ and Na_2CO_3 solutions

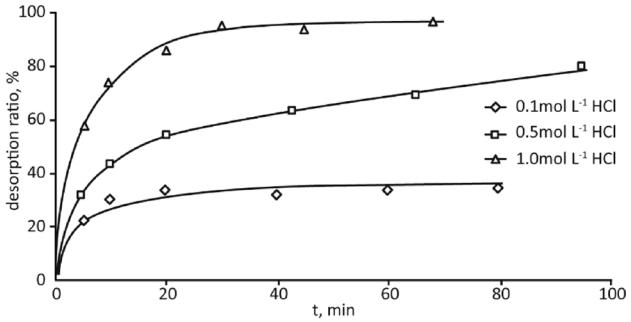

Fig. 13 Variation of desorption rate with time for different concentrations of HCl solutions. (Initial U(VI) concentration: 25 mg L^{-1}, pH 8, volume of solution 50 ml, adsorbent weight: 0.1 g, temperature: 20 °C, time: 2 h, stirring speed: 180 rpm)

As shown in Fig. 14, the adsorption amount of the synthesized fiber adsorbent did not decrease significantly until five time of use, and the decrease in the adsorption amount was observed to be large up to six cycles. Therefore, the synthesized fiber adsorbent can be recycled up to five times.

Conclusions

The adsorption process of uranium on the adsorbent was fitted to the pseudo-second-order kinetic model and the pseudo-second-order rate constant and the pseudo activation energy (44.9 kJ·mol^{-1}) were determined at different temperatures. Also, thermodynamic considerations of U(VI) adsorption process showed that adsorption was endothermic, with a value of 42.2 kJ·mol^{-1}, indicating that the adsorption was favored at higher temperatures, indicating strong interaction between the adsorbents. The process of U(VI) adsorption on the adsorbent can be considered as chemisorption. And as $\Delta S^0 = 193.8$ J·mol^{-1}·K^{-1}, the adsorption of U(VI) ions on the adsorbent shows an increase in disorder at the solid–liquid interface. Thus, it can be seen

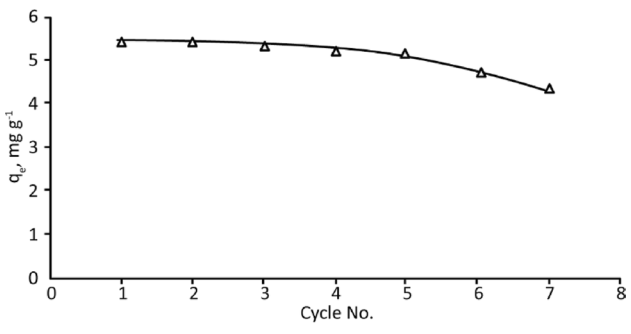

Fig. 14 Reusability of the synthesized fiber adsorbent. (Adsorption conditions: pH 8, initial uranium concentration:25 mg·L^{-1}, T = 20 °C, t = 2 h; desorption conditions: 0.5 mol L^{-1} HCl solution, T = 20 °C.)

that when the adsorption process occurs spontaneously, i.e. when $\Delta H^0 < T\Delta S^0$, the entropy change should be considered more than the enthalpy change of the adsorption process. The adsorption amount increased with pH from pH 3 to 7, and decreased slowly between pH 7 and 8, sharply between 8 and 9. The adsorption amount of U(VI) with initial U(VI) concentration was found to increase rapidly with increasing initial U(VI) concentration below 2500 $mg{\cdot}L^{-1}$, and was almost unaffected by the initial U(VI) concentration above 2500 $mg{\cdot}L^{-1}$. In particular, when the initial U(VI) concentration was 20–100 $mg{\cdot}L^{-1}$, the adsorption amount increases almost linearly with increasing initial concentration. This was due to the large number of adsorption active sites present in the adsorbent in the range of the initial U (VI) amount tested and the increase in UO_2^{2+} which can be involved in the complexation reaction with increasing temperature. The order that affects the adsorption of U(VI) was $Ca^{2+} > Mg^{2+} > Na^{+} > K^{+}$. The variation of U(VI) adsorption amount with stirring speed was not significantly affected by stirring speed from 120 rpm to above. After the adsorption of uranium on the adsorbent, it can be reused up to 5 times with 0.5 mol L^{-1} HCl solution.

Declarations

Conflict of interest Authors declare that they have no conflict of interest.

References

1. Seko N, Katakai A, Tamada M, Sugo T, Yoshii F (2005) Fine fibrous amidoxime adsorbent synthesized by grafting and uranium adsorption-elution cyclic test with seawater. Sep Sci Technol 39(16):3753–3767
2. Das S, Pandey AK, Vasudevan T, Athawale AA, Manchanda VK (2009) Adsorptive preconcentration of uranium in hydrogels from seawater and aqueous solutions. Ind Eng Chem Res 48:6789–6796
3. Zhang A, Uchiyama G, Asakura T (2003) The adsorption properties and kinetics of Uranium (VI) with a novel fibrous and polymeric adsorbent containing amidoxime chelating functional group from seawater. Sep Sci Technol 38(8):1829–1849
4. Das S, Pandey AK, Athawale A, Kumar V, Bhardwaj YK, Sabharwal S, Manchanda VK (2008) Chemical aspects of uranium recovery from seawater by amidoximated electron-beam-grafted polypropylene membranes. Desalination 232:243–253
5. Zhang A, Uchiyama G, Asakura T (2005) pH Effect on the uranium adsorption from seawater by a macroporous fibrous polymeric material containing amidoxime chelating functional group. React Funct Polym 63:143–153
6. Virendra Kumar YK, Bhardwaj KA, Dubey CV, Chaudhari NK, Goel JB, Sabharwal S (2006) Electron beam grafted polymer adsorbent for removal of heavy metal ion from aqueous solution. Sep Sci Technol 41:3123–3139
7. Caykara T, Alaslan ŞŞ, Inam R (2007) Competitive adsorption of uranyl ions in the presence of Pb(II) and Cd(II) Ions by Poly(glycidyl methacrylate) microbeads carrying amidoxime groups and polarographic determination. J Appl Polym Sci 1045:4168–4172
8. Sekiguchi K, Saito K, Konishi S, Furusaki S, Sugo T, Nobukawa H (1994) Effect of seawater temperature on uranium recovery from seawater using amidoxime adsorbents. Ind Eng Chem Res 33(662):666
9. Kavaklı PA, Seko N, Tamada M, Güven O (2004) Adsorption efficiency of a new adsorbent towards uranium and vanadium ions at low concentrations. Sep Sci Technol 39(7):1631–1643
10. Liu X, Liu H, Ma H, Cao C, Ming Yu, Wang Z, Deng Bo, Wang M, Li J (2012) Adsorption of the uranyl ions on an amidoxime-based polyethylene nonwoven fabric prepared by preirradiation-induced emulsion graft polymerization. Ind Eng Chem Res 51:15089–15095
11. Liu X, Chen H, Wang C, Qu R, Ji C, Sun C, Xu Q (2011) Adsorption properties of amidoximated porous acrylonitrile/methyl acrylate copolymer beads for Ag (I). Polym Adv Technol 22:2032–2038
12. Şimşek S, Ulusoy U (2013) Adsorptive properties of sulfolignin–polyacrylamide graft copolymer for lead and uranium: effect of hydroxylamine–hydrochloride treatment. React Funct Polym 73:73–82
13. Oyola Y, Tsouris C, Hexel CR, Mayes RT, Janke CJ, Dai S (2013) Characterization of uranium uptake kinetics from seawater in batch and flow-through experiments. Ind Eng Chem Res 52:9433–9440
14. Akperov OH, Maharramov AM, Akperov EO, Kadimova HA (2010) Novel functional polymer sorbent for adsorption of uranyl ions from aqueous solutions. Iran Polym J 19(9):717–725
15. Yu HW, Yang SS, Ruan HM, Shen JN, Gao CJ, Van der Bruggen B (2015) Recovery of uranium ions from simulated seawater with palygorskite/amidoxime polyacrylonitrile composite. Appl Clay Sci 111:67–75